CONF-9006197--1

Mechanical and Thermomechanical Stress States in Wound, Composite Rolls[1]

Received by OSTI

JUN 1 4 1990

Robert C. Reuter, Jr.

Applied Mechanics Division 1522

Sandia National Laboratories

Albuquerque, New Mexico 87185, USA

(505) 844-3136

SAND--89-2851C

DE90 012150

ABSTRACT

An analytical method is developed for calculating the mechanical and thermomechanical stress states inside orthotropic, heterogeneous, wound rolls that result from the winding process and from subsequent uniform temperature changes. Computational efficiency of the method rests on the replacement of the heterogeneous and repeated stack of layers present in the roll by a single, equivalent orthotropic layer, and treating the wound portion of the roll as an orthotropic continuum which grows during the winding process. Numerical examples are included.

NOMENCLATURE

SYMBOL	DESIGNATES	SUBSCRIPT	DESIGNATES
E	Elastic modulus	W	Layer being wound
m	Number of layer plies	E	Equivalent value
N	Number of layers	M	Mandrel
r	Variable radius	1,j,J,N	Layer indicies
R	Specific radius	i,o	Inside, outside
t	Layer or ply thickness	i,k	Summation indicies
u	Radial displacement	r,θ	Polar coordinates
ϵ	Strain		
ν	Poisson's ratio		
σ	Stress		

INTRODUCTION

Laminated, composite rolls can be fabricated by center winding multiple webs, or tapes, of different materials around a circular, cylindrical core. Direct applications for this construction include electrical capacitors with high energy density, the example chosen for this paper, magnetic switches used for current pulse compression, and various forms of structural composites. Figure 1 illustrates a capacitor being wound with simultaneous plies of aluminum conductor and mylar dielectric webs around a circular mandrel. Several supply spools are used simultaneously

[1]This work was performed at Sandia National Laboratories and supported by the U.S. Department of Energy under contract DE-AC04-76DP00789.

to provide the desired stacking sequence. As the mandrel turns, web tensions in the aluminum and mylar plies add continuously to the stress state in the growing capacitor roll until the last layer is applied. Interior stress states in the completed capacitor can have a deleterious effect on its performance. For example, high radial stresses can cause dielectric layer thinning and possible electrical failure of the capacitor. Low radial stresses in the presence of circumferential tension gradients can cause layer instabilities through bulk axial and circumferential slippage. Additionally, loss of initial winding tension in the roll interior can add significantly to the possibility of layer buckling, as examples will show. Clearly, an understanding of final stress states in these rolls and how they depend on fabrication parameters, such as web winding tensions and mandrel design, is critical to the fabrication of a reliable product. Post fabrication temperature variations (due to processing or service) can also be a factor because of the heterogeneous construction of the roll and the orthotropic behavior of many dielectric material candidates.

Problems requiring characterization of stress states in wound products fall into the general class of accreting body problems in which stressed material is continuously or incrementally added to an already stressed and deformed body. Solutions to these problems must accommodate body growth, for it is clear that the winding tensions of layers wound late in the process will influence the stress state of previously wound layers, but, the reverse is not true. Problems of this type have been treated extensively in the literature by the rolled paper (1,2), reeled tape, and prestressed pressure vessel (3) industries, however, product construction has been limited to homogeneous rolls. The present paper adds the complexity of heterogeneous construction to the analysis of stress states in wound rolls. Related work can be found in (4,5).

Two analytical approaches were considered. The first consists of incrementally adding arbitrary plies, satisfying equilibrium and compatibility conditions over all ply interfaces at each increment, and accumulating solution results. For rolls with hundreds or even thousands of plies, this can be a time consuming computational process since the number of simultaneous equations which must be solved for the solution increases with each increment, and there must be as many solutions as there are layers. A second method, that decreases computation time without significant loss of accuracy for the present application, involves development of an equivalent layer which captures the behavior of the repeated ply pattern that is wound onto the mandrel with each mandrel turn, Fig. 1. This approach drastically reduces the number of simultaneous equilibrium equations which must be solved and the compatibility conditions which must be satisfied at ply interfaces. While the number of solutions must still equal the number of layers in the completed roll, the number of layer interfaces is reduced to two (instead of $j+1$, where j varies from 1 to the total number of plies) for each increment of the solution. This computational benefit is a direct consequence of the use of an equivalent layer to represent the repeated ply pattern. Any stack of the equivalent layers is now a homogeneous continuum which grows by one layer following each solution increment. Therefore, the only interfaces at which equilibrium and compatibility must be satisfied are between the mandrel and the wound portion of the roll, and between the wound portion of the roll and the layer being wound in that increment, Fig. 2.

This paper covers derivation of the properties of the equivalent layer, development of the equations for prediction of the winding stresses and those due to uniform temperature changes throughout the roll, and reconstruction of the stress states in the plies of the equivalent layer. Numerical examples are presented and the effects of orthotropy, mandrel design and winding tension control are discussed. Stress states which could lead to undesirable physical behavior of the capacitor roll, such as layer instability, are also discussed. The entire solution is based on assumptions which include linear material behavior, incremental layer accretion, and sufficient interply friction to support ply tension variations and prevent ply slippage. Plane stress is assumed, however, plane strain can be modeled by appropriate material property substitutions. The analytical methodology presented is directly applicable to many fabrication processes which involve central winding of tapes, webs, sheets, or structural composites.

SOLUTION PRELIMINARIES

The solution method used to solve the winding and thermomechanical problems of the wound roll first requires general expressions for stress and displacement of a thick walled circular, cylindrical region. These expressions can then be specialized to represent the behavior of mandrel, wound roll, and outer layer regions, respectively, as depicted in Fig. 2. For plane stress, orthotropic, elastic behavior, constitutive and strain-displacement equations are written in cylindrical coordinates.

$$\begin{aligned}\sigma_r &= \frac{E_r}{(1-\nu_{r\theta}\nu_{\theta r})}\left[\epsilon_r + \nu_{r\theta}\epsilon_\theta - (\alpha_r + \nu_{r\theta}\alpha_\theta)\,\Delta T\right] \\ \sigma_\theta &= \frac{E_\theta}{(1-\nu_{r\theta}\nu_{\theta r})}\left[\nu_{\theta r}\epsilon_r + \epsilon_\theta - (\alpha_\theta + \nu_{\theta r}\alpha_r)\,\Delta T\right]\end{aligned} \tag{1}$$

$$\epsilon_r = \frac{du}{dr} \quad , \quad \epsilon_\theta = \frac{u}{r} \tag{2}$$

Equilibrium in the axial and polar directions is satisfied identically, while in the radial direction the following must be satisfied.

$$\frac{d\sigma_r}{dr} + \frac{(\sigma_r - \sigma_\theta)}{r} = 0 \tag{3}$$

Substitution of (2) into (1), and this result into (3) produces the following nonhomogeneous Cauchy or Euler equation which governs the problem.

$$\frac{d^2u}{dr^2} + \frac{1}{r}\frac{du}{dr} - \alpha^2\frac{u}{r^2} = \frac{\lambda}{r} \quad , \quad \alpha^2 = \frac{E_\theta}{E_r} \tag{4}$$

where

$$\lambda = -\left[\alpha_r(\nu_{r\theta}-1) - \alpha^2\alpha_\theta(\nu_{\theta r}-1)\right]\Delta T$$

Upon specifying that pressures on the inner (R_i) and outer (R_o) cylindrical surfaces of the region of interest are disignated by P_i and P_o , respectively, the general solution of (4) can be written as follows.

$$\begin{aligned} u(r) = {} & \frac{-(1-\nu_{r\theta}\nu_{\theta r})}{E_r({R_o}^{2\alpha} - {R_i}^{2\alpha})}\left[P_o {R_o}^{\alpha+1}\left(\frac{r^\alpha}{(\alpha+\nu_{r\theta})} + \frac{{R_i}^{2\alpha}}{r^\alpha(\alpha-\nu_{r\theta})}\right)\right. \\ & \left. - P_i {R_i}^{\alpha+1}\left(\frac{r^\alpha}{(\alpha+\nu_{r\theta})} + \frac{{R_o}^{2\alpha}}{r^\alpha(\alpha-\nu_{r\theta})}\right)\right] \\ & + \frac{\xi_r}{({R_o}^{2\alpha} - {R_i}^{2\alpha})}\left[\frac{(R_i R_o)^{\alpha+1}({R_o}^{\alpha-1} - {R_i}^{\alpha-1})}{r^\alpha(\alpha-\nu_{r\theta})} - \frac{r^\alpha({R_o}^{\alpha+1} - {R_i}^{\alpha+1})}{(\alpha+\nu_{r\theta})}\right] \\ & + \frac{\lambda r}{(1-\alpha^2)} \end{aligned} \tag{5}$$

where

$$\xi_r = \frac{\lambda(1+\nu_{r\theta})}{(1-\alpha^2)} - (\alpha_r + \nu_{r\theta}\alpha_\theta)\Delta T$$

Equations (5) and (2) are used with (1) to derive expressions for the radial and circumferential stress components in the cylindrical region of interest.

$$\begin{aligned}\sigma_r(r) &= \frac{-1}{({R_o}^{2\alpha} - {R_i}^{2\alpha})}\left[P_o {R_o}^{\alpha+1}\left(r^{\alpha-1} - \frac{{R_i}^{2\alpha}}{r^{\alpha+1}}\right) - P_i {R_i}^{\alpha+1}\left(r^{\alpha-1} - \frac{{R_o}^{2\alpha}}{r^{\alpha+1}}\right)\right] \\ &+ \frac{E_r\xi_r}{({R_o}^{2\alpha} - {R_i}^{2\alpha})(1-\nu_{r\theta}\nu_{\theta r})}\Big[({R_o}^{2\alpha} - {R_i}^{2\alpha}) \\ &- \left(\frac{R_i R_o}{r}\right)^{\alpha+1}({R_o}^{\alpha-1} - {R_i}^{\alpha-1}) - r^{\alpha-1}({R_o}^{\alpha+1} - {R_i}^{\alpha+1})\Big]\end{aligned} \tag{6}$$

$$\begin{aligned}\sigma_\theta(r) &= \frac{-\alpha}{({R_o}^{2\alpha} - {R_i}^{2\alpha})}\left[P_o {R_o}^{\alpha+1}\left(r^{\alpha-1} + \frac{{R_i}^{2\alpha}}{r^{\alpha+1}}\right) - P_i {R_i}^{\alpha+1}\left(r^{\alpha-1} + \frac{{R_o}^{2\alpha}}{r^{\alpha+1}}\right)\right] \\ &+ \frac{E_\theta\xi_r}{\alpha({R_o}^{2\alpha} - {R_i}^{2\alpha})(1-\nu_{r\theta}\nu_{\theta r})}\Big[\alpha({R_o}^{2\alpha} - {R_i}^{2\alpha})\frac{\xi_\theta}{\xi_r} \\ &+ \left(\frac{R_i R_o}{r}\right)^{\alpha+1}({R_o}^{\alpha-1} - {R_i}^{\alpha-1}) - r^{\alpha-1}({R_o}^{\alpha+1} - {R_i}^{\alpha+1})\Big]\end{aligned} \tag{7}$$

where

$$\xi_\theta = \frac{\lambda(1+\nu_{\theta r})}{(1-\alpha^2)} - (\alpha_\theta + \nu_{\theta r}\alpha_r)\Delta T$$

THE EQUIVALENT ORTHOTROPIC LAYER

Properties for a single, orthotropic layer that is mechanically and thermomechanically equivalent under plane stress conditions to the heterogeneous stack of plies which are wound onto the mandrel in one mandrel revolution can be determined. By enforcing equilibrium and displacement compatibility conditions in the radial and circumferential directions for the actual stack of plies and the equivalent layer, the equivalent properties can be derived. Equilibrium and compatibility equations, respectively, are given by the following.

$$\begin{aligned}\sigma_{\theta E}\sum_{i=1}^{m} t_i &= \sum_{i=1}^{m}\sigma_{\theta i} t_i \\ \sigma_{ri} &= \sigma_{rE} \quad , \quad i = 1, m\end{aligned} \tag{8}$$

$$\begin{aligned}\epsilon_{rE}\sum_{i=1}^{m} t_i &= \sum_{i=1}^{m}\epsilon_{ri} t_i \\ \epsilon_{\theta E} &= \epsilon_{\theta i} \quad , \quad i = 1, m\end{aligned} \tag{9}$$

where m is the total number of plies in the original stack. Constitutive equations of the form (1) when used in (8) and (9) above, permit derivation of the following equivalent properties.

$$E_{\theta E} = \frac{\sum_{i=1}^{m} E_{\theta i} t_i}{t_E} \quad , \quad \nu_{r\theta E} = \frac{\sum_{i=1}^{m} \nu_{r\theta i} t_i}{t_E} \quad , \quad t_E = \sum_{i=1}^{m} t_i$$

$$E_{rE} = t_E \left[\frac{\nu_{r\theta E}^2 t_E}{E_{\theta E}} + \sum_{i=1}^{m} \frac{(1-\nu_{r\theta i}\nu_{\theta r i})}{E_{ri}} \right]^{-1} \quad , \quad \nu_{\theta r E} = \frac{\nu_{r\theta E} E_{rE}}{E_{\theta E}} \tag{10}$$

$$\alpha_{\theta E} = \frac{\sum_{i=1}^{m} E_{\theta i}\alpha_{\theta i} t_i}{E_{\theta E} t_E} \quad , \quad \alpha_{rE} = \frac{1}{t_E}\sum_{i=1}^{m}(\alpha_{ri} + \nu_{r\theta i}\alpha_{\theta i})t_i - \nu_{r\theta E}\alpha_{\theta E}$$

This set of equivalent properties is available for use in the accreting continuum formulation of the winding problem and in the thermomechanical problem.

THE WINDING PROBLEM

With displacement and stress solutions of the form (5)-(7), and equivalent orthotropic properties for the repeating ply stack now available, a solution to the problems of interest can proceed. At any time during the winding process, the roll being wound can be viewed as shown in Fig. 2. As the Jth layer is being wound under a known tension, the force applied to the wound portion of the roll, and that transmitted to the mandrel, is the pressure external to the existing portion, P_J. P_J is taken as the internal pressure on the layer being wound, the Jth layer. It is assumed that this pressure exactly equilibrates the tensile stress with which the Jth layer is being wound. It is found by calculating the average value of the winding stress of the Jth layer using (7), specialized for the Jth layer, with $P_i = P_J$, $P_o = 0$, $R_i = R_J$, and $R_o = R_{J+1}$. The average winding stress in the Jth layer is given by the following.

$$\bar{\sigma}_{\theta WJ} = \frac{1}{(R_{J+1} - R_J)} \int_{R_J}^{R_{J+1}} \sigma_{\theta WJ} dr \tag{11}$$

which gives

$$P_J = \frac{\bar{\sigma}_{\theta WJ}(R_{J+1} - R_J)}{R_J} \tag{12}$$

Requiring displacement compatibility at the interface, R_1, between the mandrel and the wound portion of the roll with $P_i = P_M$ and $P_o = P_1$ for the mandrel, and $P_i = P_1$ and $P_o = P_J$ for the wound portion, allows P_1 to be written in terms of P_J, a known load.

$$P_1 = \beta_J P_J + \bar{\beta}_J \tag{13}$$

where

$$\beta_J = \frac{2\alpha\gamma_{3J} R_1^{\alpha-1} R_J^{\alpha+1}}{\gamma_{6J}(\alpha^2 - \nu_{r\theta}^2)}$$

$$\begin{aligned} \bar{\beta}_J = {} & \frac{2\alpha R_M^{\alpha_M+1} R_1^{\alpha_M-1} P_M}{\gamma_{6J}(\alpha_M^2 - \nu_{r\theta M}^2)} + \frac{\gamma_{4J}}{\gamma_{6J}} \left[\frac{R_J^{\alpha+1}(R_J^{\alpha-1} - R_1^{\alpha-1})}{(\alpha - \nu_{r\theta})} - \frac{R_1^{\alpha-1}(R_J^{\alpha+1} - R_1^{\alpha+1})}{(\alpha + \nu_{r\theta})} \right] \\ & - \frac{\gamma_1}{\gamma_{6J}} \left[\frac{R_M^{\alpha_M+1}(R_1^{\alpha_M-1} - R_M^{\alpha_M-1})}{(\alpha_M - \nu_{r\theta M})} - \frac{R_1^{\alpha_M-1}(R_1^{\alpha_M+1} - R_M^{\alpha_M+1})}{(\alpha_M + \nu_{r\theta M})} \right] + \frac{(\gamma_5 - \gamma_2)}{\gamma_{6J}} \end{aligned}$$

$$\gamma_1 = \frac{E_{rM}\xi_{rM}}{(1 - \nu_{r\theta M}\nu_{\theta r M})} \quad , \quad \gamma_2 = \frac{E_{rM}\lambda_M(R_1^{2\alpha_M} - R_M^{2\alpha_M})}{(1-\alpha^2)(1 - \nu_{r\theta M}\nu_{\theta r M})} \tag{14}$$

$$\gamma_{3J} = \frac{E_{rM}(R - 1^{2\alpha_M} - R_M^{2\alpha_M})(1 - \nu_{r\theta M}\nu_{\theta r M})}{E_r(R_J^{2\alpha} - R_1^{2\alpha})(1 - \nu_{r\theta}\nu_{\theta r})}$$

$$\gamma_{4J} = \frac{E_{rM}\xi_r(R_1^{2\alpha_M} - R_M^{2\alpha_M})}{E_r(R_J^{2\alpha} - R_1^{2\alpha})(1-\nu_{r\theta}\nu_{\theta r})} \quad , \quad \gamma_5 = \frac{E_{rM}\lambda(R_1^{2\alpha_M} - R_M^{2\alpha_M})}{(1-\alpha^2)(1-\nu_{r\theta}\nu_{\theta r})}$$

$$\gamma_{6J} = \gamma_{3J}\left[\frac{R_1^{2\alpha}}{(\alpha+\nu_{r\theta})} + \frac{R_J^{2\alpha}}{(\alpha-\nu_{r\theta})}\right] - \left[\frac{R_1^{2\alpha_M}}{(\alpha_M+\nu_{r\theta M})} + \frac{R_M^{2\alpha_M}}{(\alpha_M-\nu_{r\theta M})}\right]$$

Expressions (12) and (13), when used with (5)-(7) specialized for the region of interest, allow final calculation of displacements and stresses in that region that are a result of incrementally adding the Jth layer. Thermal terms are carried along to this point for use in subsequent calculations.

To complete the analysis of the mechanical states caused by winding, the thermal terms are now disregarded and the mechanical terms, induced by P_J of Fig. 2, are retained. Final stresses in the mandrel after the last layer has been wound are obtained by summing the stress contributions of all layers wound. Likewise, final stresses in any layer of the wound portion of the roll, the ith layer, are obtained by summing its winding stress and the incremental stresses induced by the winding of subsequent layers. Results are given by the following expressions specialized for the mandrel, wound portion, and the final layer, respectively.

$$\begin{aligned} \sigma_{rM}(r) &= \frac{-(r^{2\alpha_M} - R_o^{2\alpha_M})}{(R_1^{2\alpha_M} - R_o^{2\alpha_M})}\left(\frac{R_1}{r}\right)^{\alpha_M+1}\sum_{k=1}^{J}\beta_k P_k \\ \sigma_{\theta M}(r) &= \frac{-\alpha_M(r^{2\alpha_M} + R_o^{2\alpha_M})}{(R_1^{2\alpha_M} - R_o^{2\alpha_M})}\left(\frac{R_1}{r}\right)^{\alpha_M+1}\sum_{k=1}^{J}\beta_k P_k \end{aligned} \qquad (15)$$

where $J = 1, N$

$$\begin{aligned} \sigma_{rj}(r) &= \frac{P_j R_j^{\alpha+1}}{(R_{j+1}^{2\alpha} - R_j^{2\alpha})}\left(r^{\alpha-1} - \frac{R_{j+1}^{2\alpha}}{r^{\alpha+1}}\right) \\ &\quad - \sum_{k=j+1}^{J}\frac{P_k R_k^{\alpha+1}}{(R_k^{2\alpha} - R_1^{2\alpha})}\left[\left(r^{\alpha-1} - \frac{R_1^{2\alpha}}{r^{\alpha+1}}\right) - \beta_k\left(\frac{R_1}{R_k}\right)^{\alpha+1}\left(r^{\alpha-1} - \frac{R_k^{2\alpha}}{r^{\alpha+1}}\right)\right] \\ \sigma_{\theta j}(r) &= \frac{\alpha P_j R_j^{\alpha+1}}{(R_{j+1}^{2\alpha} - R_j^{2\alpha})}\left(r^{\alpha-1} + \frac{R_{j+1}^{2\alpha}}{r^{\alpha+1}}\right) \\ &\quad - \alpha\sum_{k=j+1}^{J}\frac{P_k R_k^{\alpha+1}}{(R_k^{2\alpha} - R_1^{2\alpha})}\left[\left(r^{\alpha-1} + \frac{R_1^{2\alpha}}{r^{\alpha+1}}\right) - \beta_k\left(\frac{R_1}{R_k}\right)^{\alpha+1}\left(r^{\alpha-1} + \frac{R_k^{2\alpha}}{r^{\alpha+1}}\right)\right] \end{aligned} \qquad (16)$$

where $J = 2, N$ and $R_j \le r \le R_{j+1}$

$$\begin{aligned} \sigma_{rJ}(r) &= \frac{P_J R_J^{\alpha+1}}{(R_{J+1}^{2\alpha} - R_J^{2\alpha})}\left(r^{\alpha-1} - \frac{R_{J+1}^{2\alpha}}{r^{\alpha+1}}\right) \\ \sigma_{\theta J}(r) &= \frac{\alpha P_J R_J^{\alpha+1}}{(R_{J+1}^{2\alpha} - R_J^{2\alpha})}\left(r^{\alpha-1} + \frac{R_{J+1}^{2\alpha}}{r^{\alpha+1}}\right) \end{aligned} \qquad (17)$$

where $J = 1, N$

The winding process progresses by letting J vary from 1 (the first layer wound) to N (the last layer wound). Equations (16) permit stress calculations for the jth layer after J layers have been wound, subject to $j \le J$. Note that when $J = 1$, there is no wound portion of the roll, and Eqs. (16) are not required. Also of interest is the average circumferential stress in the jth layer of the wound portion of the roll, since it can be compared directly to the original winding stress of that layer. Integrating the second of Eqs. (16) with an equation of the form (11) gives the following result.

$$\bar{\sigma}_{\theta j} = \bar{\sigma}_{\theta W j} - \frac{1}{(R_{j+1}^{\alpha} - R_j^{\alpha})} \sum_{k=j+1}^{J} \bar{\sigma}_{\theta W k} \left[R_k^{\alpha} \left(1 + \left(\frac{R_1^2}{R_j R_{j+1}} \right)^{\alpha} \right) + \frac{\beta_k R_1^{\alpha+1}}{R_k} \left(1 + \left(\frac{R_k^2}{R_j R_{j+1}} \right)^{\alpha} \right) \right] \quad (18)$$

where $J = 2, N$

THE THERMOMECHANICAL PROBLEM

Once the winding process is completed, the finished roll may be exposed to uniform temperature changes during subsequent processing, texting, or service. Returning to Eqs. (12), (13), and (5)-(7), retaining the thermal terms, and disregarding the mechanical terms due to winding stresses gives the following expressions for radial and circumferential thermal stress due to uniform temperature changes in the completed roll.

$$\begin{aligned} {}_T\sigma_{rj}(r) &= \frac{\bar{\beta}_{N+1} R_1^{\alpha+1}}{(R_{N+1}^{2\alpha} - R_1^{2\alpha})} \left(r^{\alpha-1} - \frac{R_{N+1}^{2\alpha}}{r^{\alpha+1}} \right) + \frac{E_r \xi_r}{(R_{N+1}^{2\alpha} - R_1^{2\alpha})(1 - \nu_{r\theta}\nu_{\theta r})} \Big[(R_{N+1}^{2\alpha} - R_1^{2\alpha}) \\ &\quad - \left(\frac{R_1 R_{N+1}}{r} \right)^{\alpha+1} (R_{N+1}^{\alpha-1} - R_1^{\alpha-1}) - r^{\alpha-1}(R_{N+1}^{\alpha+1} - R_1^{\alpha+1}) \Big] \\ {}_T\sigma_{\theta j}(r) &= \frac{\alpha \bar{\beta}_{N+1} R_1^{\alpha+1}}{(R_{N+1}^{2\alpha} - R_1^{2\alpha})} \left(r^{\alpha-1} + \frac{R_{N+1}^{2\alpha}}{r^{\alpha+1}} \right) + \frac{E_\theta \xi_r}{\alpha (R_{N+1}^{2\alpha} - R_1^{2\alpha})(1 - \nu_{r\theta}\nu_{\theta r})} \Big[\frac{\xi_\theta \alpha (R_{N+1}^{2\alpha} - R_1^{2\alpha})}{\xi_r} \\ &\quad + \left(\frac{R_1 R_{N+1}}{r} \right)^{\alpha+1} (R_{N+1}^{\alpha-1} - R_1^{\alpha-1}) - r^{\alpha-1}(R_{N+1}^{\alpha+1} - R_1^{\alpha+1}) \Big] \end{aligned} \quad (19)$$

where $R_j \leq r \leq R_{j+1}$.

The average circumferential thermal stress in the jth layer is given by

$$\begin{aligned} {}_T\bar{\sigma}_{\theta j} &= \frac{\bar{\beta}_{N+1} R_1^{\alpha+1} (R_{j+1}^{\alpha} - R_j^{\alpha})}{(R_{N+1}^{2\alpha} - R_1^{2\alpha})(R_{j+1} - R_j)} \left(1 + \left(\frac{R_{N+1}^2}{R_j R_{j+1}} \right)^{\alpha} \right) + \frac{E_\theta}{(1 - \nu_{r\theta}\nu_{\theta r})} \Big[\xi_\theta \\ &\quad + \frac{\xi_r (R_{j+1}^{\alpha} - R_j^{\alpha})}{\alpha^2 (R_{N+1}^{2\alpha} - R_1^{2\alpha})(R_{j+1} - R_j)} \left[\frac{(R_1 R_{N+1})^{\alpha+1} (R_{N+1}^{\alpha-1} - R_1^{\alpha-1})}{(R_j R_{j+1})^{\alpha}} - (R_{N+1}^{\alpha+1} - R_1^{\alpha+1}) \right] \Big] \end{aligned} \quad (20)$$

PLY STRESS RECONSTRUCTION

The winding and thermomechanical problem solutions thus far are based on the response of the equivalent layer which is made up of the individual plies that are wound onto the roll in one mandrel revolution. Since it is of most interest to know the stress states in the individual plies of the equivalent layer, reconstruction of their values from the equivalent layer solution is necessary. This is accomplished by summing strain values in the ith ply of the jth layer due to initial winding, due to being wound over by subsequent layers, and due to uniform temperature changes. Stress values are then calculated by substituting these strain values into the appropriate ply constitutive relation of the form (1). Results are given by the following.

$$\epsilon_{rij} = -\frac{\nu_{r\theta j} \bar{\sigma}_{\theta W j}}{E_{\theta i}} + \frac{\bar{\sigma}_{rj}}{E_{ri}} - \frac{\nu_{r\theta i} (\bar{\sigma}_{\theta j} - \bar{\sigma}_{\theta W j})}{E_{\theta E}}$$

$$
\begin{aligned}
{}_T\epsilon_{rij} &= \frac{{}_T\bar{\sigma}_{ri}}{E_{ri}} - \frac{{}_T\bar{\sigma}_{\theta i}\nu_{r\theta i}}{E_{\theta E}} + \alpha_{ri}\Delta T \\
\epsilon_{\theta ij} &= \frac{\bar{\sigma}_{\theta W j}}{E_{\theta i}} + \frac{(\bar{\sigma}_{\theta j} - \bar{\sigma}_{\theta W j})}{E_{\theta E}} - \frac{\nu_{r\theta i}\bar{\sigma}_{rj}}{E_{\theta i}} \\
{}_T\epsilon_{\theta ij} &= \frac{{}_T\bar{\sigma}_{ri} - \nu_{r\theta i}}{E_{\theta i}} + \frac{{}_T\bar{\sigma}_{\theta i}}{E_{\theta E}} + \alpha_{\theta i}\Delta T \\
\sigma_{rij} &= \bar{\sigma}_{rj} \\
{}_T\sigma_{rij} &= {}_T\bar{\sigma}_{ri} \\
\sigma_{\theta ij} &= \bar{\sigma}_{\theta W j} + \frac{E_{\theta i}}{E_{\theta E}}(\bar{\sigma}_{\theta j} - \bar{\sigma}_{\theta W j}) \\
{}_T\sigma_{\theta ij} &= \left(\frac{E_{\theta i}}{E_{\theta E}}\right) {}_T\bar{\sigma}_{\theta i}
\end{aligned}
\qquad (21)
$$

This completes the winding and thermomechanical problem solutions.

NUMERICAL EXAMPLE

Eight ply, 260 turn construction of a capacitor wound on a 0.312 inch diameter, solid, paper phenolic mandrel provides the numerical example. The following geometric and material properties apply.

Material	Ply No.	E_r (psi)	E_θ (psi)	$\nu_{r\theta}$	α_r (/deg C)	α_θ (/deg C)	t (in)
Aluminum	2,6	$1 \cdot 10^7$	$1 \cdot 10^7$	0.33	$2.32 \cdot 10^{-5}$	$2.32 \cdot 10^{-5}$	$2 \cdot 10^{-4}$
Mylar	1,3,4,5,7,8	$2.5 \cdot 10^4$	$6.4 \cdot 10^5$	0.17	$3.4 \cdot 10^{-5}$	$1.7 \cdot 10^{-5}$	$4 \cdot 10^{-4}$
Paper Phenolic	–	$1 \cdot 10^6$	$1 \cdot 10^6$	0.4	$3.6 \cdot 10^{-5}$	$3.6 \cdot 10^{-5}$	–

The aluminum and mylar plies, which are 2 inches wide, are wound with 0.5 lb and 0.36 lb constant winding tensions, respectively. Of interest are the radial stresses throughout the capacitor, and the circumferential tensions (not stresses) in the two different ply materials. Results are presented for the winding process only, followed by a uniform temperature rise of 75 deg C, as determined by Eqs. (16a), (18), (19a), and (20). Winding tensions are obtained by simply multiplying circumferential stresses by ply cross sectional areas. Winding results, thermomechanical results, and their sums are presented in Figs. 3 - 8.

RESULTS AND DISCUSSION

Circumferential (wound) tensions and radial stresses resulting from the winding phase of fabrication are represented as the solid lines in the figures. There is significant loss of initial winding tension throughout most of the wound roll, particularly in the aluminum plies. In the interior of the roll, adjacent mylar and aluminum plies experience about the same radial motion due to being overwrapped, and since the aluminum material is so much stiffer than mylar, it undergoes higher tension losses. There is a steep gradient in wound tension of the aluminum plies near the mandrel, a region which could be the sight of circumferential slippage due to the inability of contact friction between adjacent plies to support large tension changes. Also, most of the aluminum plies throughout the roll have actually been driven into compression, a mechanical state which is conducive to buckling. Wound tensions in all plies approach their winding tension values at the outer radius of the roll. Radial stresses are compressive throughout the wound roll, with peek values at the mandrel interface. As the wound tension decreases, so does the radial stress which equilibrates it. Radial stresses should be sufficiently high to hold the roll together, however, not so high that dielectric dimensions change significantly.

A uniform temperature rise causes internal stresses which, when added to the wound stress states, increase tension gradients near the mandrel, increase tension losses in the aluminum plies, decreases tension losses in the mylar plies, and substantially increases maximum radial stress values. Heating the capacitor roll, therefore, increases the threat of 1. roll slippage near the mandrel, 2. aluminum ply buckling, and 3. excessive dielectric material thinning. Cooling the wound roll reverses some of these trends, as seen in Figs. 6 - 8. Tension losses are increased in mylar plies and decreased in most aluminum plies, and radial stresses are reduced. Note also that wound tension loss in aluminum plies near the mandrel has increased, sufficiently in fact to cause radial stresses near the mandrel to become tensile. This condition is not possible, however, since the ply/ply and ply/mandrel interfaces cannot support tension. Therefore, with sufficient cooling, it is possible to cause a serious roll stability problem by separating the roll from the mandrel.

CLOSURE

A method for calculating the mechanical stress states in wound rolls of heterogeneous construction has been developed. This method has been presented in a way to permit its extension to the calculation of thermomechanical stresses which arise from a uniform temperature change. The numerical example provided insights to potential problems of an actual capacitor which could effect product performance and reliability. Additional work is needed to improve the quality and accuracy of these calculations, particularly with regard to material modeling. While the whole theory was cast in the light of its principal application, the wound capacitor, the methodology is applicable to other wound products, including the more traditional structural composite construction.

REFERENCES

1. Altmann, H.C., "Formulas for Computing the Stresses in Center-Wound Rolls." The Journal of the Technical Association of the Pulp and Paper Industry, Vol. 51, No. 4, 1968, pp 176-179.
2. Yogoda, H.P., "Resolution of a Core Problem in Wound Rolls," ASME Journal of Applied Mechanics, Vol. 47, 1980, pp 847-854.
3. Rasty, J. and Sabbaghian, M., "Effect of Imperfect Contact Between Adjacent Layers on the Integrity of Wrapped Vessels," ASME Journal of Pressure Vessel Technology, Vol. 110, 1988, pp 247-254.
4. Reuter, R.C., Jr. and Allen, J.J., "Mechanical States in Wound Capacitors Part I - Prediction," to be published in the ASME Journal of Mechanical Design.
5. Allen, J.J. and Reuter, R.C., Jr., "Mechanical States in Wound Capacitors Part II - Optimization," to be published in the ASME Journal of Mechanical Design.

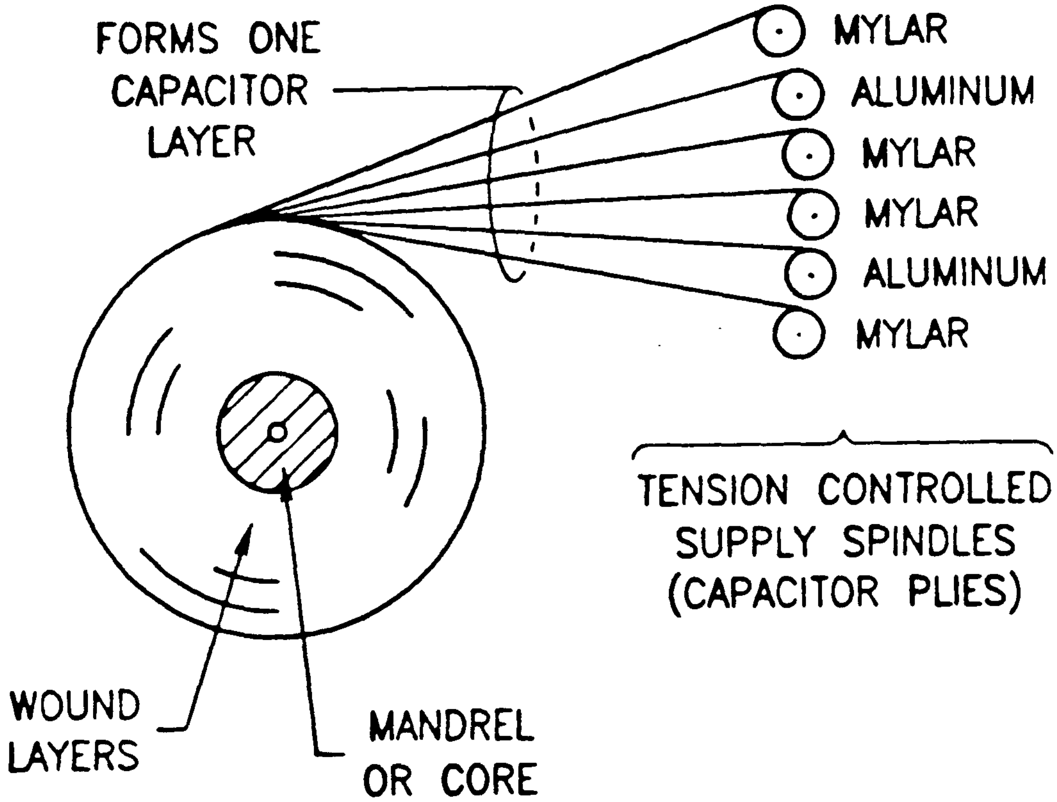

Figure 1. Capacitor winding.

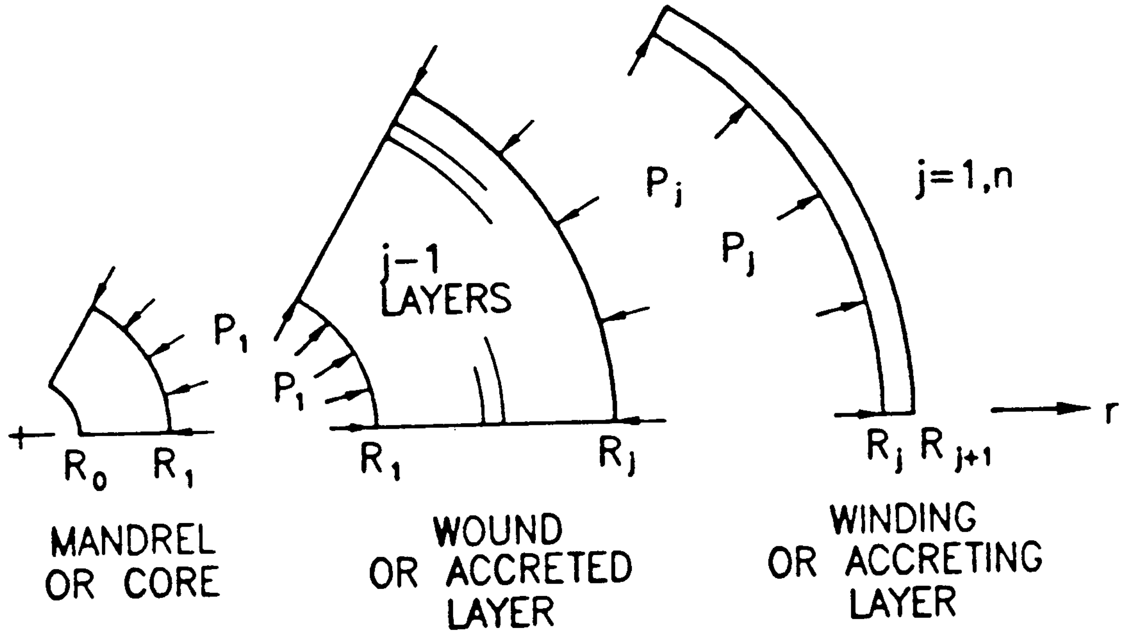

Figure 2. Capacitor anatomy.

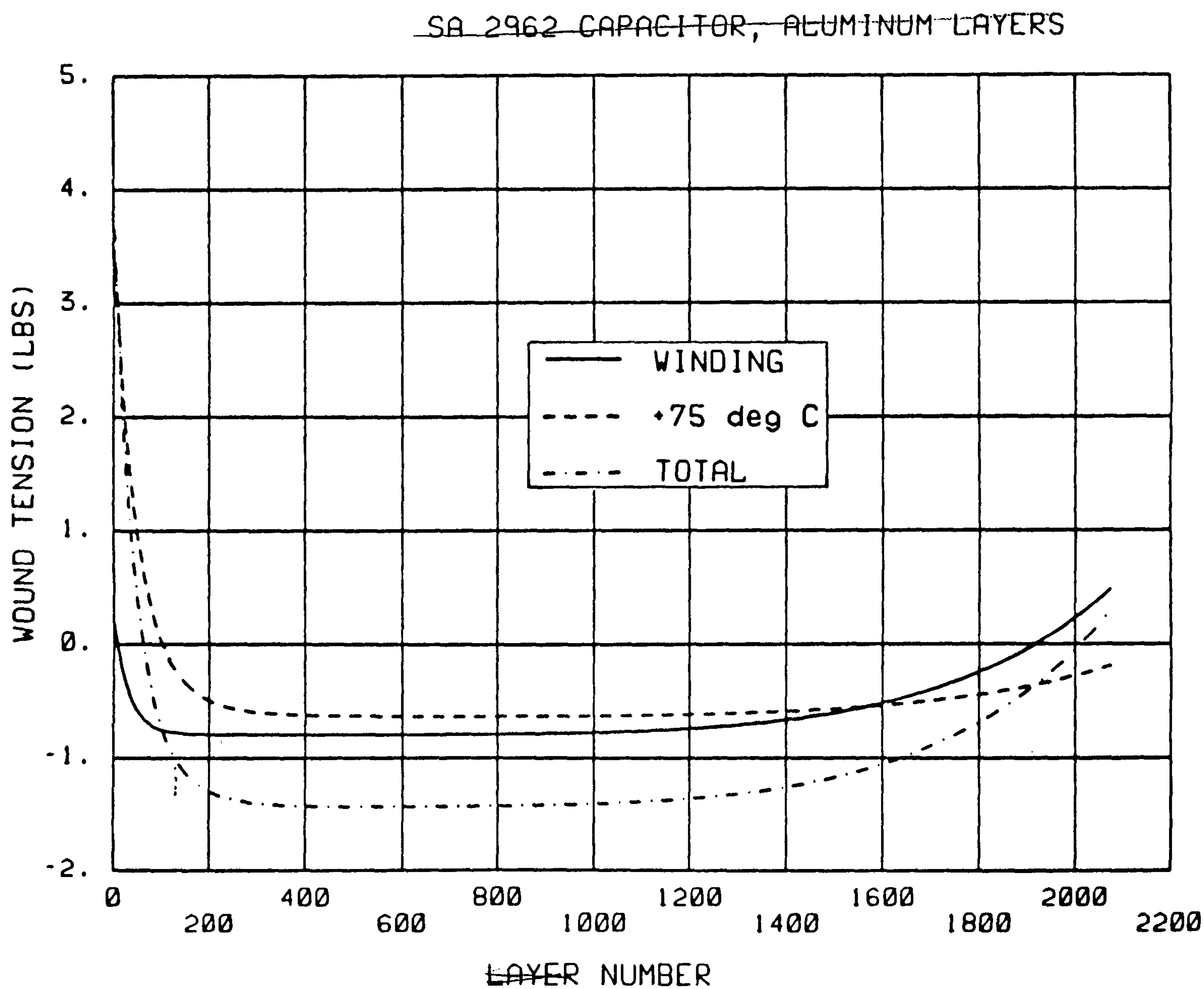

Fig. 3

GRAFAID 5.0 15-FEB-1990 13:11

SA 2962 CAPACITOR, MYLAR LAYERS

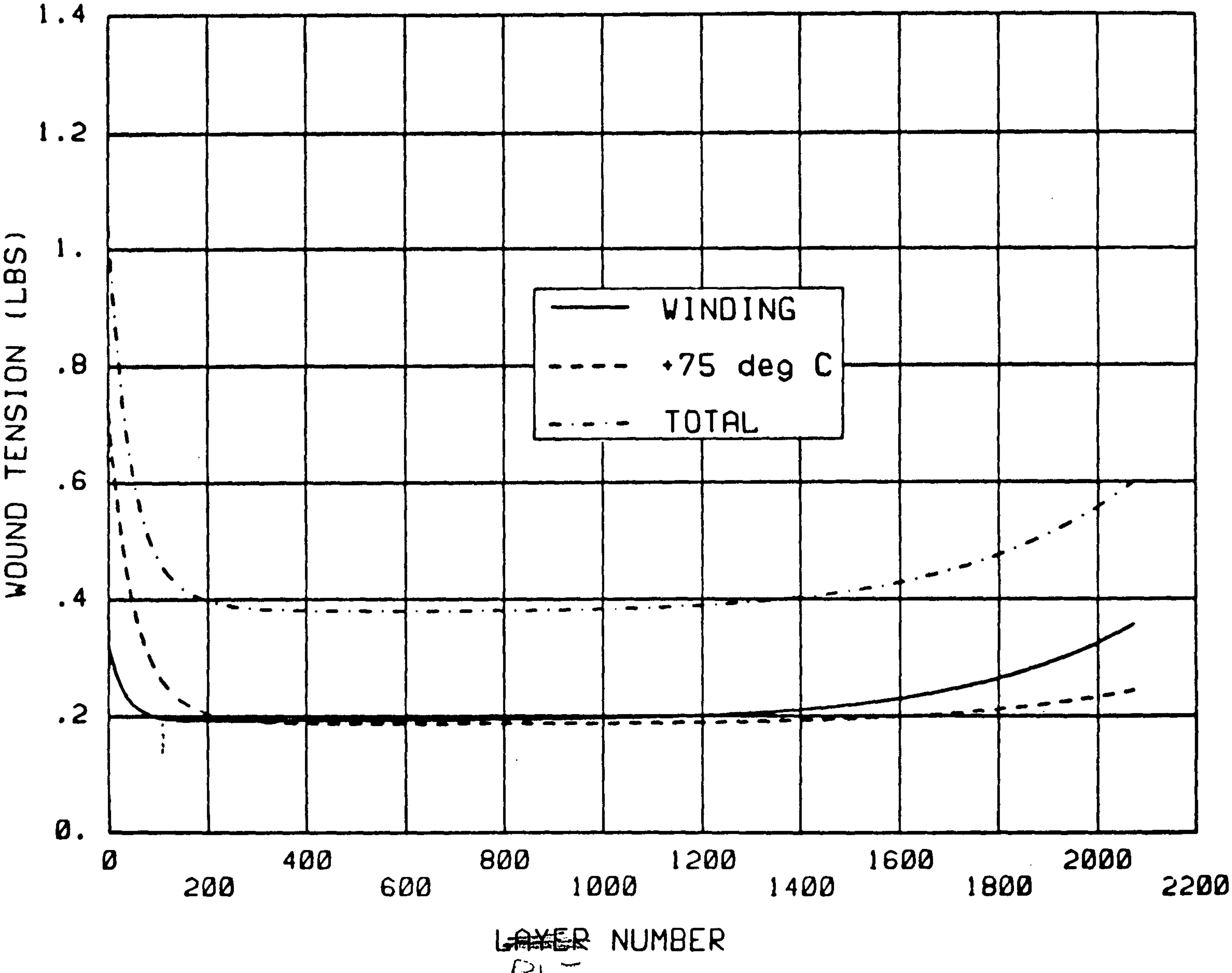

Fig 4

GRAFAID 3.0 15-FEB-1990 12:47

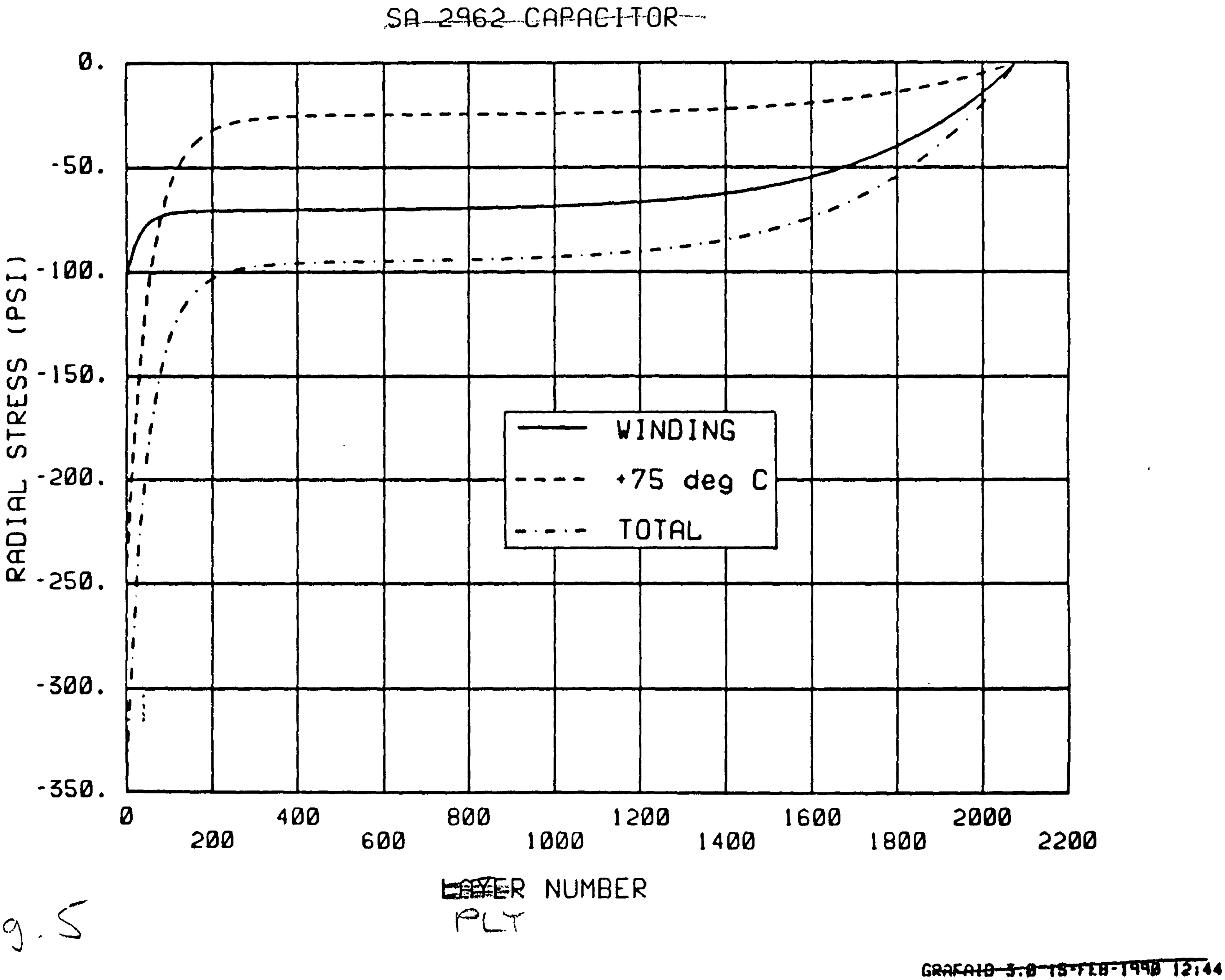
SA 2962 CAPACITOR
RADIAL STRESS (PSI)
0.
-50.
-100.
-150.
-200.
-250.
-300.
-350.
0
200
400
600
800
1000
1200
1400
1600
1800
2000
2200
WINDING
+75 deg C
TOTAL
LAYER NUMBER
PLT
GRAFAID 3.0 15-FEB-1990 12:44

Fig. 5

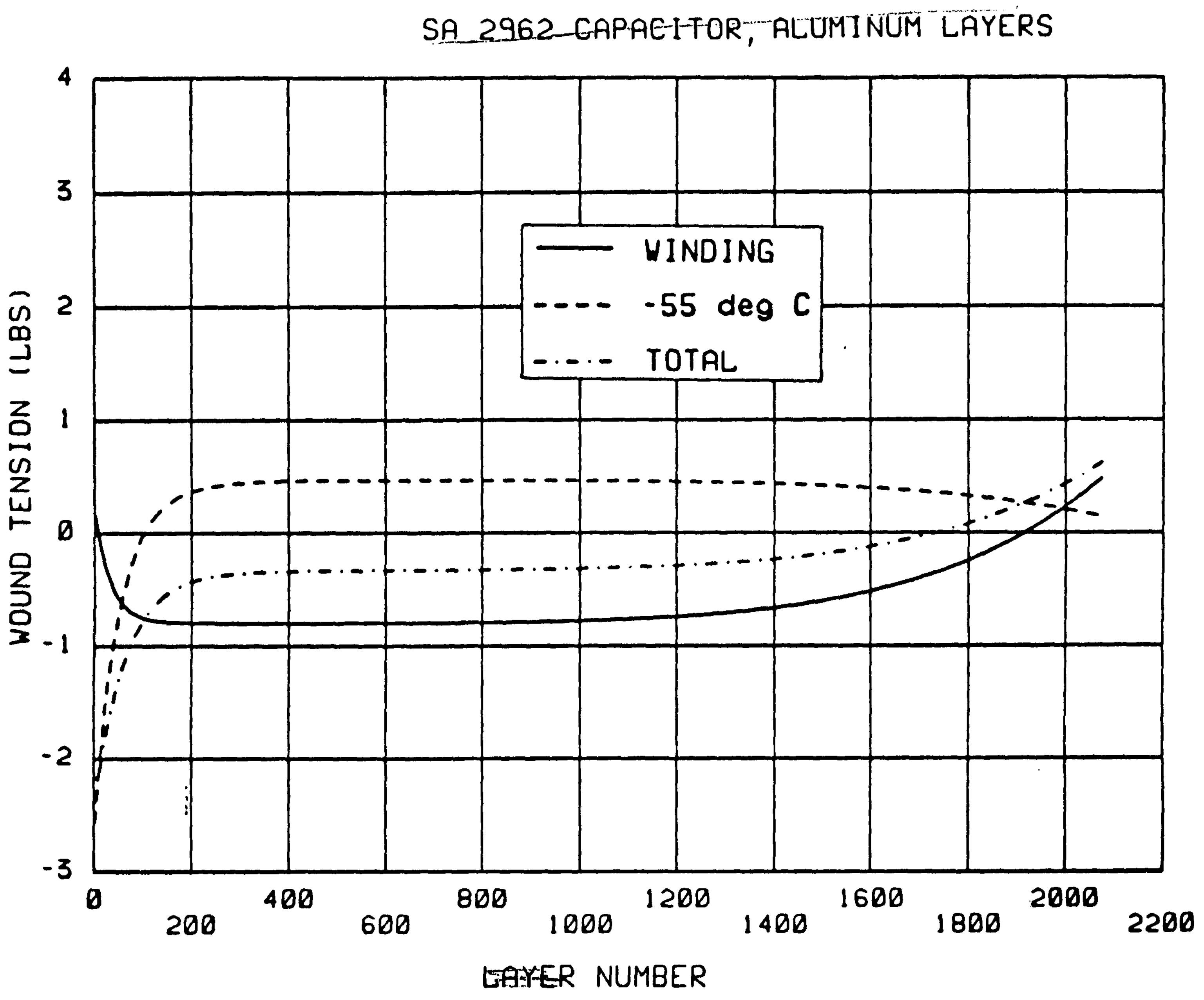

Fig 6

PLT

GRAFAID-3.0-16-FEB-1990 07:10

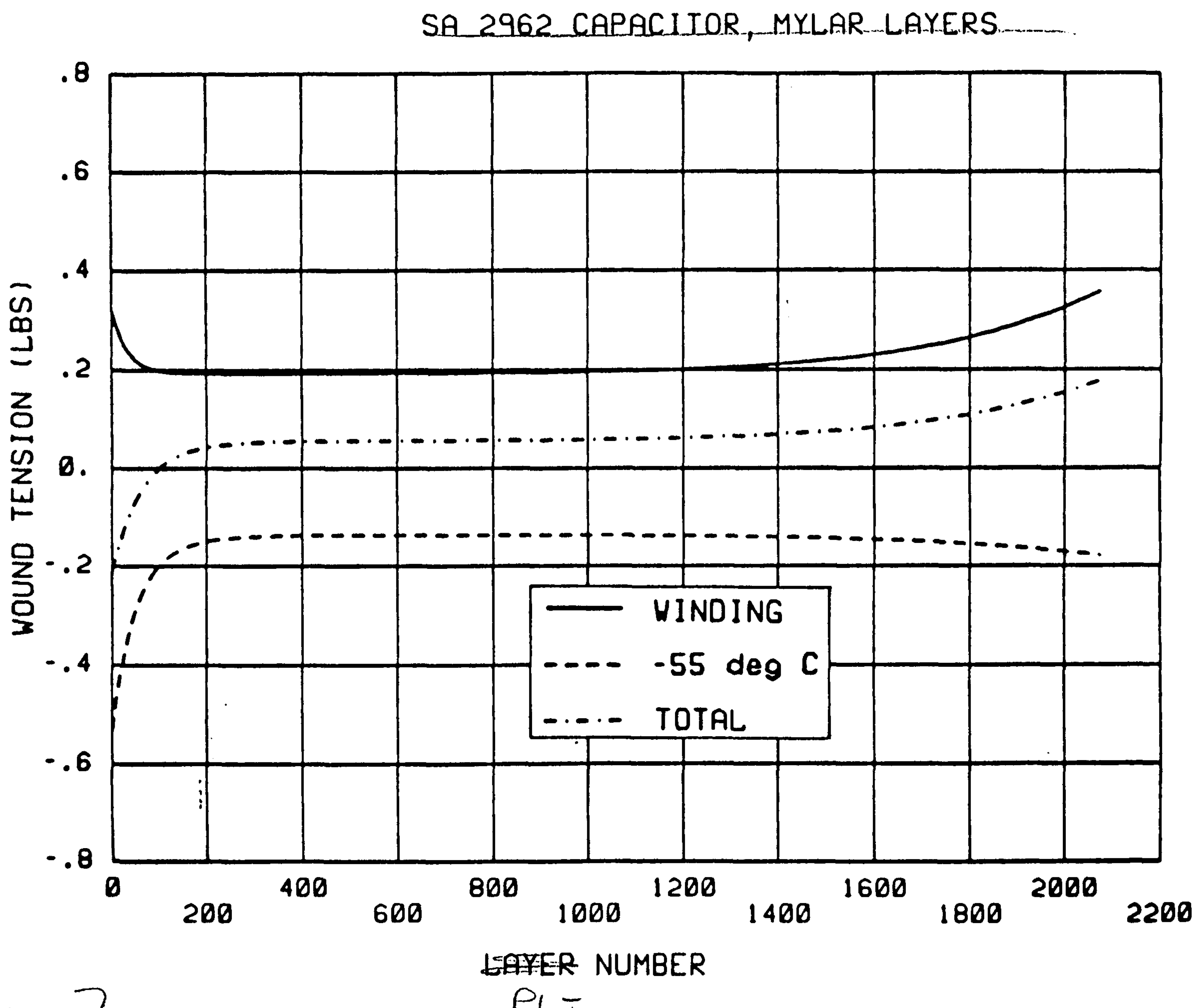

Fig-7

GRAFAID 5.0 16-FEB-1990 07:23

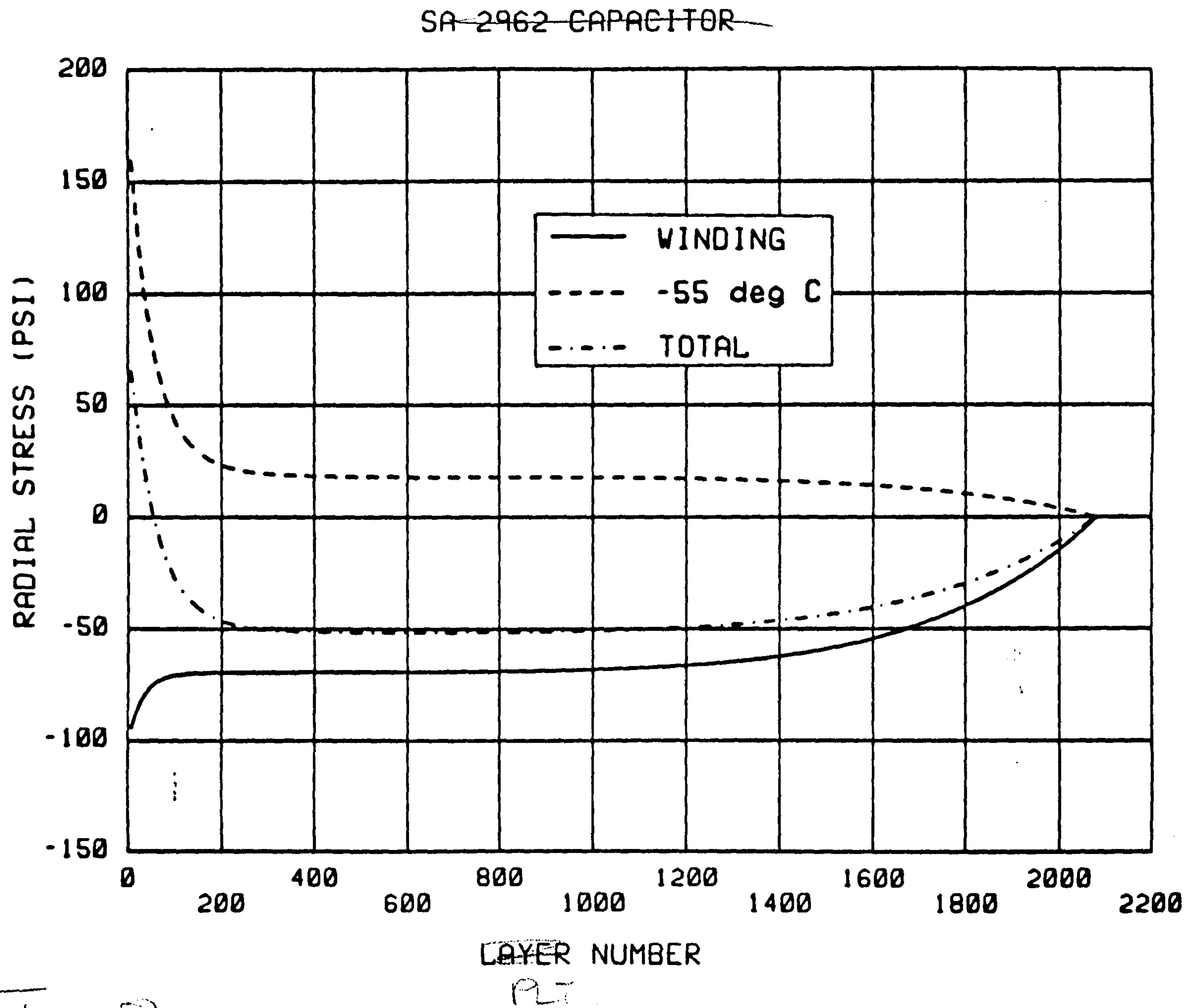

Fig. 8

GRAFAID 3.0 16-FEB-1990 07:20